Water Research 221 (2022) 118795

Contents lists available at ScienceDirect

Water Research

journal homepage: www.elsevier.com/locate/watres

Quantification of polyhydroxyalkanoate accumulated in waste activated sludge

Ruizhe Pei [a,b,*], Gerard Vicente-Venegas [b], Mark C.M. Van Loosdrecht [a], Robbert Kleerebezem [a], Alan Werker [b]

[a] Department of Biotechnology, Delft University of Technology, Van der Maasweg 9, Delft 2629 HZ, the Netherlands
[b] Wetsus, European Centre of Excellence for Sustainable Water Technology, Oostergoweg 9, Leeuwarden 8911 MA, the Netherlands

ARTICLE INFO

Keywords:
Polyhydroxyalkanoate (PHA)
Biopolymer
Activated sludge
Staining
Image analysis
Thermogravimetric analysis (TGA)

ABSTRACT

Polyhydroxyalkanoate accumulation experiments at pilot scale were performed with fullscale municipal waste activated sludge. Development of biomass PHA content was quantified by thermogravimetric analysis. Over 48 h the biomass reached up to 0.49 ± 0.03 gPHA/gVSS (n = 4). Samples were processed in parallel to characterise the distribution of PHA in the biomass. Selective staining methods and image analysis were performed by Confocal Laser Scanning Microscopy. The image analysis indicated that nominally 55% of this waste activated sludge was engaged in PHA storage activity. Thus even if the biomass PHA content reached 0.49gPHA/gVSS, the accumulating fraction of the biomass was estimated to have attained about 0.64gPHA/gVSS. The combination of quantitative microscopy and polymer mass assessment enabled to distinguish the effect of level of enrichment in PHA storing bacteria and the average PHA storage capacity of the accumulating bacteria. The distribution of microbial 16S rRNA levels did not follow a measurable trend during PHA accumulation.

1. Introduction

Polyhydroxyalkanoates (PHA) are polyesters that can be accumulated as intracellular granules by many types of microorganisms especially under dynamic environmental conditions (Anderson and Dawes, 1990; Dawes and Senior, 1973; Van Loosdrecht et al., 1997). Typically, these dynamic conditions are created by alternating the presence and absence of organic carbon sources and/or electron acceptors. Under dynamic conditions, PHA accumulation is a competition strategy for microorganisms to thrive (Majone et al., 1999; Reis et al., 2003; Van Loosdrecht et al., 1997). The accumulated intracellular polymers can be harvested and applied as biobased and biodegradable polyesters. PHAs are functional and suitable in many kinds of applications compared to fossil oil derived polyesters used ubiquitously today (Laycock et al., 2013; Pratt et al., 2019).

Microbial community-based PHA production processes exploit purposefully imposed or inherently present environmental conditions in open microbiological processes that favour the growth and enrichment of PHA storing phenotypes (Estevez-Alonso et al., 2021; Kleerebezem and van Loosdrecht, 2007; Kourmentza et al., 2017). Depending on the source of the PHA-storing biomass, microbial community-based PHA production methods may be denoted as either *enrichment accumulation* or *direct accumulation* approaches. *Enrichment accumulation* refers to PHA production with a biomass that has been produced purposefully with optimised selection conditions. A majority of the selected bacteria in the biomass is expected to produce PHA. A *direct accumulation* process uses waste activated sludge produced in municipal and/or industrial biological wastewater treatment plants (WWTPs) (Bengsston et al., 2017; Morgan-Sagastume, 2016). Notwithstanding that the principal function of the process is to treat wastewater, selection of PHA-storing microorganisms will occur due to the inherent dynamic process conditions (Van Loosdrecht et al., 1997). The selection could be due to the cyclic day-night loading regime in wastewater supply and/or a plug flow character in the wastewater treatment process (Werker et al., 2020). The wastewater treatment processes select for a microbial community that has broad functional diversity. As a result, there will be non-PHA storing microorganisms in the *direct accumulation* biomass essential for the treatment of influent contaminants (Pei et al., 2022).

PHA production is accomplished in a side-stream fed-batch bioprocess where the supplied PHA-storing biomass is fed with volatile fatty acid rich substrates to reach the maximum biomass PHA content. The volatile fatty acid rich substrates can be derived for example from the

* Corresponding author at: Department of Biotechnology, Delft University of Technology, Van der Maasweg 9, Delft 2629 HZ, the Netherlands.
E-mail address: r.pei@tudelft.nl (R. Pei).

https://doi.org/10.1016/j.watres.2022.118795
Received 28 April 2022; Received in revised form 23 June 2022; Accepted 24 June 2022
Available online 25 June 2022

fermentation of wastewater, organic fraction of municipal solid waste or the primary sludge of a WWTP (Estevez-Alonso et al., 2021). The use of fermented primary sludge also offers the possibility of converting the WWTP into a PHA production facility without modifying the main treatment process. Over the past 10 years, different pilot scale studies demonstrated the technical feasibility of microbial community-based PHA production processes using different feedstocks (Estevez-Alonso et al., 2021).

In the PHA production process, maximum biomass PHA content is a critical performance factor that influences the economic viability of commercial advancements (Estevez-Alonso et al., 2021; Paul et al., 2020; Valentino et al., 2017). Consequently, in almost all the microbial community-based research literature to date, maximum achievable biomass PHA content has been a key parameter when assessing the performance of the PHA production process. Biomass PHA content is typically quantified by the mass of PHA accumulated with respect to the total volatile suspended solids (VSS). Active biomass is commonly approximated by the VSS minus the PHA mass in these solids. Microbial community-based approaches have been reported to have a maximum biomass PHA content between 30 and 90% gPHA/gVSS (Estevez-Alonso et al., 2021). Implicitly it is often assumed that improvement in PHA production is reflected by improvement in selection and mitigating flanking populations during accumulation (Tamis et al., 2014).

Observed different biomass PHA content for microbial community-based approaches may be attributed to two main factors. One factor is the fraction of PHA-storing bacteria in the biomass defined as a degree of enrichment. The other factor is the PHA accumulation capacity of the active PHA-storing bacteria. The current methods for measurement of biomass PHA content do not provide insight to distinguish between these two factors. To assess the individual cellular PHA distribution, flow cytometry or Raman spectroscopy may be applied. In pure cultures, Nile red or BODIPY staining has been employed with flow cytometry to quantify the PHA content and to study the PHA content in single cells (Kacmar et al., 2006; Saranya et al., 2012; Vidal-Mas et al., 2001). Similarly, methods have been explored based on floc disruption and statistics of cell-to-cell PHA content by means of Raman spectroscopy of the dispersed microbial biomass (Majed et al., 2009). In microbial community-based PHA research, these methods are less applicable due to problems of dispersion of the biomass in single cells and the variation of cellular morphologies in microbial communities. Moreover destruction of the floc structure obscures to obtain information from the distribution of the PHA granules and PHA-storing bacteria in the communities.

The aim of the present work is to develop the selective staining methods for a quantitative estimation of the municipal activated sludge degree of enrichment and, consequently, the average PHA accumulation capacity of the PHA storing fraction of that biomass. In the present work, the PHA-rich biomass was produced with a municipal activated sludge using the *direct accumulation* approach at pilot scale. The progress of polymer accumulation was monitored over time with grab samples for biomass PHA content. Recently developed selective staining for visualisation on parallel samples was also applied (Pei et al., 2022). Obtained Confocal Laser Scanning Microscopy (CLSM) images were analysed to quantify the PHA distribution.

2. Material and methods

2.1. PHA Accumulation methods and sampling

A well-mixed 200 L jacketed stainless steel reactor with 167 L working volume for PHA accumulation was operated as described previously (Pei et al., 2022). The accumulation feedstock was acetic acid (20 gCOD/L) with added NH_4Cl and KH_2PO_4 (VWR, the Netherlands) to a COD:N:P of 100:1:0.05 (by weight). The feedstock was adjusted to pH 5.0±0.5 with NaOH pellets (VWR, the Netherlands). The substrate was supplied in a fed-batch feed-on-demand process controlled according to biomass respiration response monitored (JUMO ecoLine O-DO, JUMO GmbH & Co. KG, Germany) by dissolved oxygen trend as described in Werker et al. (2020). The source biomass that was evaluated for the purposes of the this study was gravity belt thickened (nominally 5.5% total solids) waste activated sludge from WWTP Bath, the Netherlands.

Thickened activated sludge was diluted with tap water to target 2.5gVSS/L and brought to operating temperature (25 °C) in the active working volume. Aeration and mixing were up to 12 h until steady state dissolved oxygen levels indicated a steady biomass endogenous respiration level. This pre-aeration was followed by acclimation applied as a sequence of three feast-famine cycles (Morgan-Sagastume et al., 2017). At the beginning of the feast period, a pulse of substrate that targeted a reactor acetic acid concentration of 100 mgCOD/L was given. For each feast-famine cycle, the length of the feast and famine period was approximately 20 and 60 min, respectively. After the third famine phase, pulse wise feed-on-demand PHA accumulation was performed over 48 h with constant mixing and aeration (Pei et al., 2022). Substrate doses in pulse wise inputs targeted a maximum reactor acetic acid concentration of 100 mgCOD/L.

At selected time points 4 x 50 mL representative mixed liquor grab samples were taken. Duplicate sub-samples of 5 mL were fixed with formaldehyde to a final concentration of 3.7% (Sigma-Aldrich, Netherlands), preserved in 10 mL 1X phosphate buffered saline (PanReac AppliChem, ITW Reagents, Spain) with 10 mL pure ethanol (VWR, the Netherlands), and stored at 5 °C before performing the staining. Afterwards, the remaining fixed sample was stored at -20 °C for long-term preservation.

2.2. Analytical methods

Mixed liquor sample volumes were measured (V). Mixed liquor suspended solids were separated by centrifugation (3248RCF and 4 °C for 20 m), and the supernatant was removed. The pellet mass was transferred with Milli-Q water (Merck, Germany) by rinsing into a clean pre-dried (105 °C) and tare weighed crucible. The pellet mass (m_1) representing total suspended solids (TSS) was estimated from the dried weight (105 °C over 12 h). Afterwards, pellet fixed solids (m_2) were determined by ashing at 550 °C for 2 h. The mixed liquor VSS concentration was estimated as $(m_1 - m_2)/V$.

Biomass PHA content was determined by thermogravimetric analysis (TGA) according to Chan et al. (2017) with minor modification. The mixed liquor sample was acidified to nominally pH 2 with 98% H_2SO_4 (VWR, the Netherlands), mixed (10 min), and then centrifuged (3248RCF and 4 °C for 20 m). The pellet was dried (105 °C overnight) and milled to a powder after decanting supernatent. About 5 mg of powder samples were disposed to thermal decomposition (TGA 2, Meller Toledor, Switherlands) in 3 principal steps as follows: 1) isothermal nitrogen gas atmosphere drying at 105 °C for 10 min; 2) heating with nitrogen gas atmosphere at 10° / min to 550 °C; 3) isothermal ashing in air atmosphere at 550 °C for 30 min.

The biomass PHA content as gPHA / gVSS was derived from the background corrected characteristic polymer decomposition peak detectable from the derivative thermogravimetric trend as described in Chan et al. (2017) using in-house Matlab data processing algorithms (MathWorks, MA, USA). Non-PHA biomass was estimated as VSS minus PHA mass. Subsequently, the mass ratio of PHA and non-PHA biomass was calculated.

2.3. Biomass staining and microscopy image analysis

For the samples fixed with formaldehyde, intracellular PHA granules and protein staining was performed using BODIPY 493/503® (BODIPY) (Thermo Fisher Scientific, MA, USA) in combination with SYPRO™ Red (Thermo Fisher Scientific, MA, USA) as described in Pei et al. (2022). Glass slides with 10 reaction wells (Paul Marienfeld GmbH & Co.KG, Germany) were used. In each reaction well, 5 μL fixed sample was

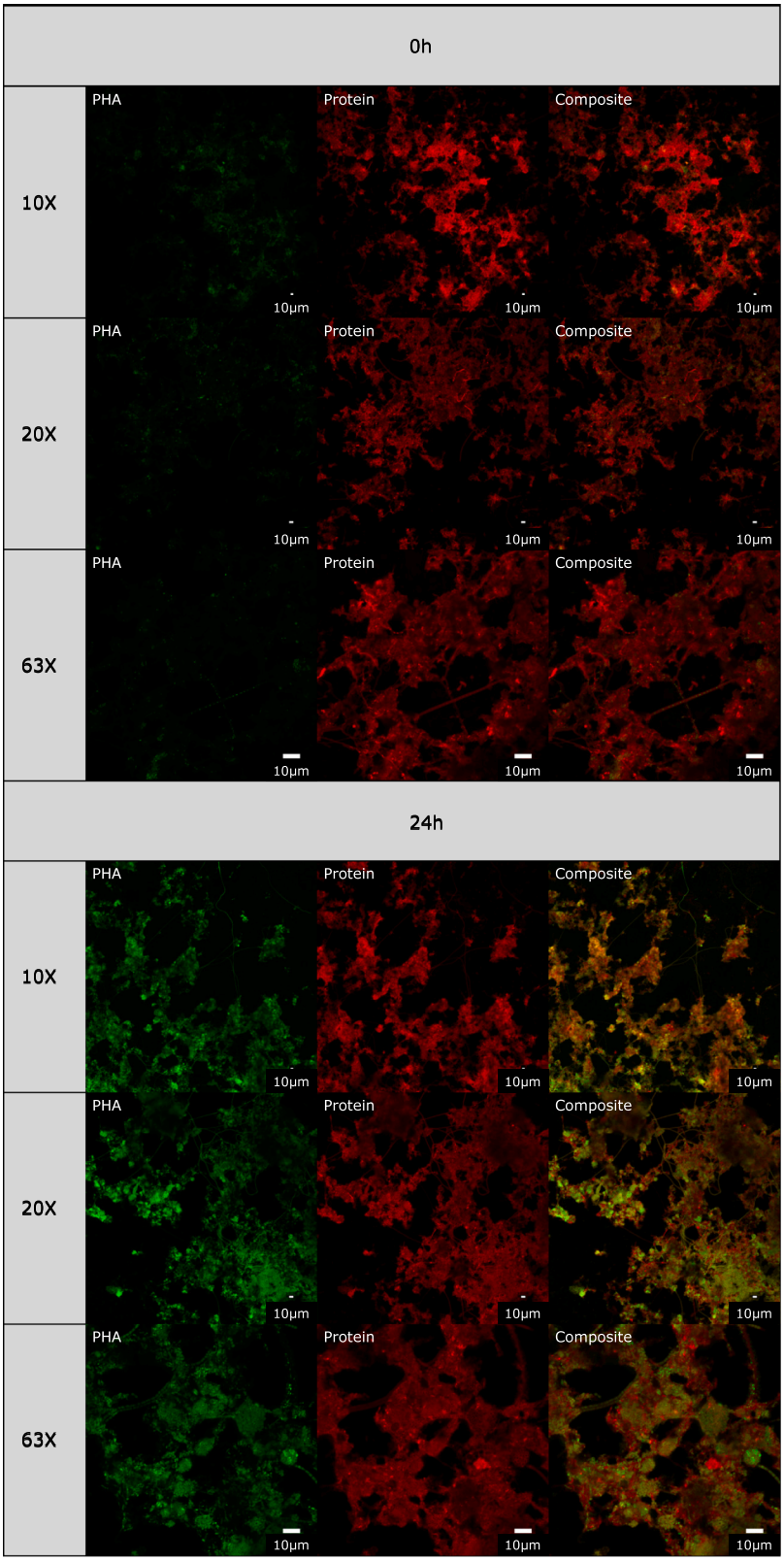

Fig. 1. Activated sludge after 0 h and 24 h accumulation staining image channels for PHA (green) and protein (red), plus the composite image at 10X, 20X and 63X magnifications. (For interpretation of the references to colour in this figure legend, the reader is referred to the web version of this article.)

loaded with 0.5 μL BODIPY at 2 ng/μL and 0.5 μL of 100 times diluted SYPRO Red. The loaded slides were incubated at 46 °C until dried. The dried slide was washed with Milli-Q water to remove any excess dye and then dried again with compressed air. Each prepared slide was mounted with VECTASHIELD® HardSet™ Antifade Mounting Medium H-1400-10 (Vectashield) (Vector Laboratories, CA, USA) and sealed.

For the same series of the fixed samples, Fluorescence *In-situ* Hybridization (FISH) using the bacterial probe EUB338-I (5' GCT GCC TCC

CGT AGG AGT3') labelled with Cy5 was combined with PHA staining via BODIPY and DNA staining with DAPI. The staining was performed according to Llobet-Brossa et al. (1998) with modifications as described in Pei et al. (2022). A 0.5 μL aliquot fixed sample was heat fixed in a slide well then dehydrated with ethanol. Hybridization buffer, 10 μL with 35% formamide, was added followed by 0.5 μL of EUB 338I, BODIPY and DAPI at, respectively, 50 ng/μL, 2 ng/μL and 250 ng/μL. The hybridization was performed at 46 °C for 1.5 h followed by washing using buffer pre-heated to 48 °C for 15 m and cold Milli-Q water. The washed slide was dried with compressed air, then mounted and sealed with Vectashield.

The Confocal Laser Scanning Microscope LSM 880 (Carl Zeiss, Germany) was used with Plan-Apochromat 10X/0.45 M27, 20X/0.8 M27 and 63X/1.4 Oil DIC objectives (Carl Zeiss, Germany). From each sample well, with 63X objective, a sequence of 11 randomly selected images with floc containing fields of view were acquired (digital resolution 1584 by 1584 pixel for the images with 2 dyes and 1912 pixel by 1912 pixel for the images with 3 dyes) after initially surveying the well for sample quality. Dyes were excited and dye specific captured images averaged from 16 scans were saved to separate file channels at 16 bit depth. To excite DAPI, BODIPY, SYPRO Red and Cy5, a Diode 405-30 laser at 405 nm, an Argon laser at 488 nm, a DPSS 561-10 laser at 561 nm and a HeNe633 laser at 633 nm were used, respectively. The same laser power and gain were used for each dye in each respective set of 11 images taken, and imaging conditions were otherwise kept similar from well-to-well.

Fiji Image J (ImageJ2, Ver 1.52P) was used for processing the captured images. Brightness levels were maximized without over-exposing pixel data. Then for each dye specific channel with each respective well-series of 11 images, a cut off threshold intensity level was established by visual inspection. Total pixel areas of BODIPY, SYPRO Red, RNA FISH and DAPI were measured representing areas/bio-volume of PHA, proteins, 16S rRNA, and DNA.

2.4. Data analysis and interpretation

The trends in progress of biomass PHA content (gPHA/gVSS) over time were estimated by least-squares regression analysis according to Bengsston et al. (2017):

$$\text{Biomass PHA Content} = A_0 + A_1\left(1 - e^{-t/\tau}\right) \quad (1)$$

where A_0 and A_1 are constants that enable the estimation of rates as a function of time. The accumulation time constant τ (h) represented process first order kinetics in reaching a maximum level of PHA content.

From microscopy and image analysis, a characteristic relative area ratio for PHA to non-PHA biomass ratio (v/v) was calculated:

$$\text{PHA to non-PHA Biomass ratio (v/v)} = \frac{\text{PHA Area}}{\text{Non-PHA Biomass Area}} \quad (2)$$

where the overlay of PHA pixel area distribution on flocs were evaluated from the BODIPY signal. The non-PHA biomass area could be assessed from protein or DNA related fluorescent signals, namely Protein Area, and DNA Area.

Relative signal pixel distributions in overlay areas defined by the individual biomass flocs were used to give an index representing the fraction of the viable microorganisms as:

$$\text{Viable Microorganism Fraction} = \frac{\text{RNA Area}}{\text{DNA Area}} \quad (3)$$

Similarly, an index representing a measure for the PHA-storing microorganism fraction within the expressed viable areas for flocs within each captured field of view was characterized as:

$$\text{Viable PHA-storing Microorganism Fraction} = \frac{\text{PHA Area}}{\text{RNA Area}} \quad (4)$$

In order to impose a normal distribution for statistical analysis, the obtained v/v ratios were transformed to a logit scale (Warton and Hui, 2011):

$$x' = ln\frac{x}{1-x} \quad (5)$$

where x is the v/v ratios of PHA to non-PHA Biomass, Viable Microorganism Fraction and Viable PHA-storing Microorganism Fraction obtained by Eqs. (2)–(4), and x' is the respective transformed v/v ratios.

The statistical analysis including one way ANOVA, Pearson's Chi-square normality test, quantile-quantile plot, and linear regression were performed in the logit scale. The averages and the standard deviations for the ratios (Eqs. (2)–(4)) were calculated with the logit transformed results (x'). Final results are reported with values transformed back to the scale of proportions (0–1):

$$X = \frac{10^{x'}}{10^{x'} + 1} \quad (6)$$

where x' is the average v/v ratios of PHA to non-PHA Biomass, Viable Microorganism Fraction and Viable PHA-storing Microorganism Fraction in the logit scale.

3. Results and discussion

The potential for quantitative image analysis was evaluated from replicated accumulation experiments for the reproducibility and selection of image magnification. The PHA accumulation process performance was assessed by the biomass PHA content development (Eq. (1)). From the optimal magnification, correlation between volume and mass ratios of PHA to non-PHA biomass was established. The degree of enrichment of PHA-storing bacteria for activated sludge from Bath WWTP was estimated. Subsequently, from the estimated biomass PHA content and the degree of enrichment, the average biomass PHA content for the PHA-storing fraction in the activated sludge was calculated. Combined staining of PHA, FISH and DNA was applied to monitor the trend of microbial activity during the PHA accumulation process.

3.1. Quantification of PHA distribution

Previously methods of selective staining were developed and applied to visualise the PHA storage process (Pei et al., 2022). Efforts to extend methods for quantitative image analysis started with the assessment of reproducibility alongside considerations for optimal image magnification. For the CSLM system, available objectives with 10, 20 and 63X magnification using optimum settings with 2 image channels, represented image pixel dimensions of 0.26, 0.15 and 0.09 μm/pixel, respectively. Replicate slides (n = 3) were prepared with 4 replicate wells per slide on biomass samples with negligible polymer content (0 h accumulation) and with significant polymer content (24 h accumulation). For each well, 4 to 11 fields of view were acquired at the three available magnifications Fig. 1. Less images were acquired with 10X magnification compared to 63X where 11 images were taken due to floc concentration and differences in coverage. This dataset was used to evaluate quantitative reproducibility.

The pixel area of PHA is expected to be proportional to an integrated volume of PHA defined by the magnification dependent pixel area and CSLM focal depth. Similarly, the volume of non-PHA biomass is expected to be proportional to the protein area or DNA area identified with SYPRO Red or DAPI, respectively. These volumes relate to mass by respective densities of the biomass and PHA granules. If the densities remain constant during the accumulation process then the PHA to non-PHA biomass volume to volume ratio (v/v) from image analysis should

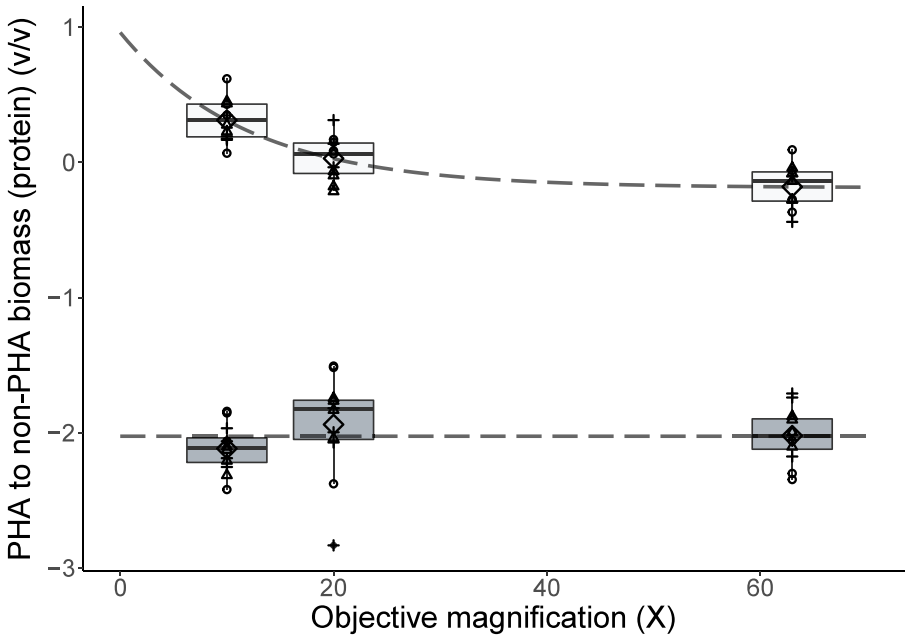

Fig. 2. Box plot of volume ratio (Eq. (2)) of PHA to non-PHA biomass (protein) for activated sludge in the logit scale after 0 h (gray) and 24 h (white) accumulation with pooled results from replicate slides ($n = 3$) with 4 measurement wells on each slide, and 11 fields of view for each well with 10X, 20X and 63X magnification. The average volume ratio of PHA to non-PHA biomass (protein) for each slide 1, 2, 3 and the ensemble average are represented by ◯, △, + and ◆, respectively.

correspond directly with the PHA to non-PHA biomass mass to mass ratio (m/m) provided by TGA analysis. However, the mass ratio can range from 0 to infinity while the volume ratio derived from overlapping respective pixel areas from image analysis is constrained to range from 0 to 1. This constrained range also affects the normality of the obtained results (Warton and Hui, 2011). To make the correlation between the volume ratio and the mass ratio, a logit transformation (Eq. (5)) was applied to the data of image analysis to account for the inherently bounded scale.

After the logit transformation, the reproducibility of the volume ratio between the area of PHA and non-PHA biomass represented by the area of protein stain was assessed. For initial samples (0 h) or samples after accumulation (24 h), one way ANOVA of the averaged PHA and non-PHA biomass (protein) volume ratio per reaction well indicated no significant difference (95% CI) for analysis of replicate wells ($n = 4$) on the same slide. Similarly, no significant difference (95% CI) was found among the reaction wells among three replicate slides. This outcome suggested that one well with a representative sample could describe the average state of the biomass during an accumulation if sufficient fields of view are acquired per well. Consistent outcomes between replicate slides supported potential for the quantitative reproducibility of the methods of staining and image analysis.

Influences of magnification on the observation of PHA-rich biomass were first assessed qualitatively. Details of interest including individual bacterial cells and PHA granules were anticipated to be in the order of 1 μm and 0.5 μm, respectively. As shown in Fig. 1, the applied magnification for analysis did not strongly influence outcomes of image analysis at the beginning of an accumulation, because biomass PHA content is low at start. Even with 10X magnification, the morphology of microorganisms and the floc structures were clearly visible. After 24 h, with a pronounced degree of PHA accumulation, resolution of PHA with respect to biomass pixel areas was dependent on the magnification (Fig. 1). A lower magnification provides a greater observation area with greater depth of field but PHA granules and individual cells were not well-resolved. With increasing magnification from 0.26 μm/pixel to 0.09 μm/pixel resolution, boundaries between cells and even between

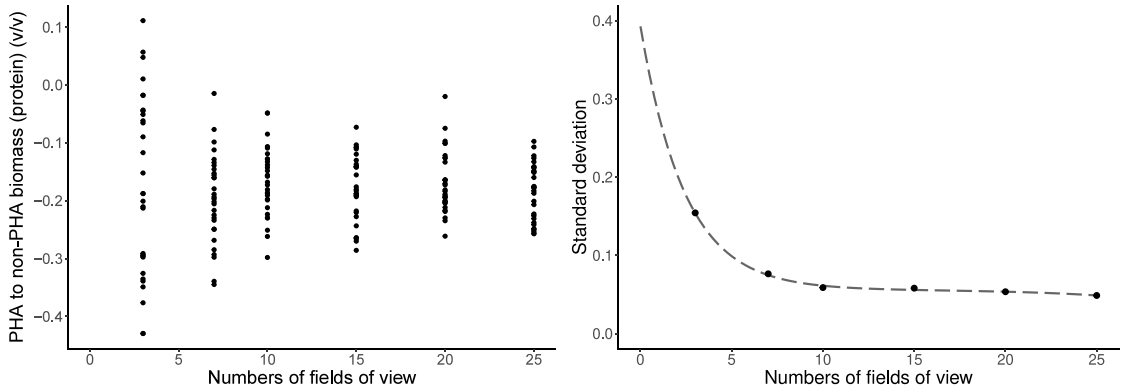

Fig. 3. The Monte Carlo simulated average volume ratio of PHA to non-PHA biomass (protein) **(a)** and standard deviation of the simulated volume ratio of PHA to non-PHA biomass (protein) **(b)** using random selection (3, 7, 10, 15, 20 and 25 fields of view) of the pooled replicate data for 63X magnification and accumulated activated sludge after 24 h.

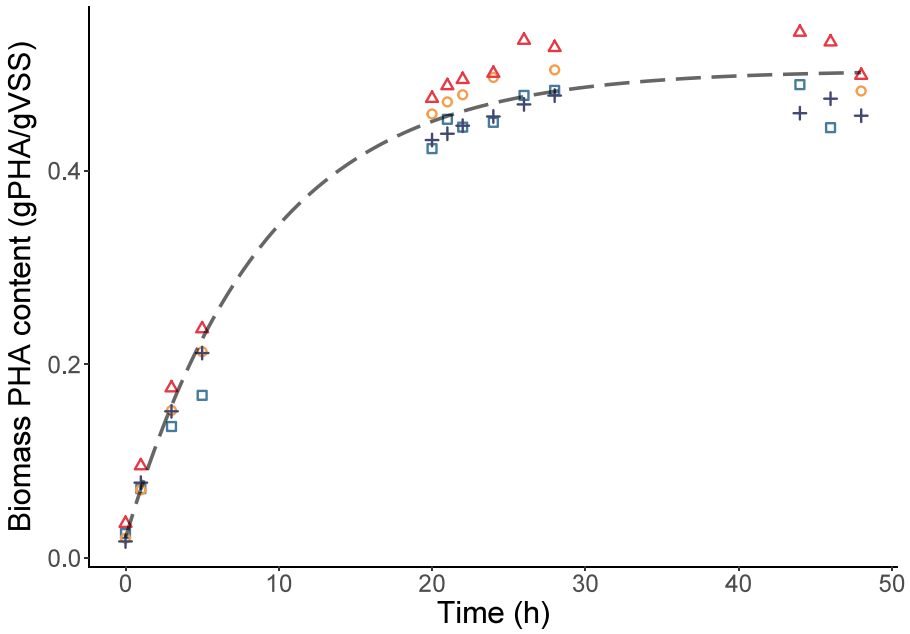

Fig. 4. TGA measured biomass PHA content at different time point in 4 PHA accumulation replicated runs. Blue□, yellow ◯, red △ and purple + represent Run1, Run2, Run3 and Run4, respectively. The dash line ($y = 0.02 + 0.48 \times (1 - e^{-t/9.1})$) is the PHA content trend on average from 4 experiments with Eq. (1).

the intracellular PHA granules became increasingly more discernible. For example, considering filamentous microorganisms (Fig. 1) the area occupied by PHA is smaller than biomass area defined by protein staining. It was observed that with lower magnification, interpreted extracellular polymeric substances surrounding flocs diffuse the signal by scattering signal from PHA. This reduced image quality and resulted in harder to determine area boundaries.

The potential for an influence from magnification on the quantitative image analysis was considered (Fig. 2). At low biomass PHA content, even if average values may suggest a drift of underestimation, one way ANOVA results on the logit scale suggested no significant difference of the means (95% CI). For the PHA-rich biomass after 24 h accumulation, the average volume ratio of PHA to non-PHA biomass (protein) on the logit scale suggests a trend of a significant overestimation at lower magnification (DF=2, Residue= 26, $F = 27.48$, $p < .001$). Such bias may be due to pixel areas over representing the underlying PHA granule area with the decreased resolution. The normality of the PHA to non-PHA biomass volume ratio of 24 h samples obtained with different magnifications was tested using Pearson's Chi-square test. The ratios obtained when using 63X objective ($p = .67$) showed a better normality compared to 10X ($p = .07$) and 20X ($p = .02$) objectives were used. Therefore, considering the resolution and the outcomes for a normal distribution of the obtained results, 63X magnification was selected in subsequent development for a quantitative analysis.

A disadvantage of using higher magnification for the image acquisition and quantitative analysis was that each field of view captures a smaller absolute area. Due to an observed heterogeneity in floc to floc PHA granule distribution, sufficient fields of view were required towards obtaining a representative average value (Pei et al., 2022). Monte Carlo simulation was performed for random selection of the pooled replicate data for 63X magnification and 24-h accumulation (Fig. 3). Results of Monte Carlo simulation, Fig. 3(a) suggested an increasing number of fields of view estimated PHA to non-PHA biomass ratios distributed in smaller ranges. Fig. 3(b) shows the standard deviation of the simulated results given in Fig. 3(a) when using different numbers of fields of view. The standard deviation indicated that increasing the acquired number of fields of view resulted in progressive reduction in the uncertainty of an estimated volume ratio of PHA to non-PHA biomass (protein). The trend suggests that for 63X magnification, at least 10 fields of view were required for reaching a low and steady standard deviation. When the numbers of fields of views increased from 3 to 10, the standard deviation decreased from 0.15 to 0.06. When the numbers of fields of view further increased from 10 to 20, the standard deviation decreased from 0.06 to 0.05. Considering the trade off between the workload, the benefits, and the necessary redundancy, 11 fields of view were implemented in the following sections for a robust estimate of the average v/v distribution in the biomass.

3.2. PHA Accumulation processes performance

To assess if the staining method could follow the development of the PHA accumulation process quantitatively, 4 replicate 48-h PHA accumulation experiments were conducted and evaluated. As shown in Fig. 4, the trends of TGA measured biomass PHA content exhibited the robust performance with minor differences in accumulation extent even for these different batches of full-scale waste activated sludge collected on different days over 5 weeks. The trend in biomass PHA content development in time could be described according to Eq. (1) with A_0, A_1 and τ equal to 0.02 gPHA/gVSS, 0.48 gPHA/gVSS and 9.1 h with the standard errors of 0.009, 0.010 and 0.720, respectively (on average with pooled data). From this development it was estimated that the biomass PHA content became essentially constant by 27 h (3τ). An average estimated biomass PHA content in replicate accumulations after 27 h was 0.49±0.03 gPHA/gVSS. The average maximum biomass PHA content was similar to what has been previously reported for this particular activated sludge (Bengtsson et al., 2017). The average observed yield on substrate from the 4 accumulation experiments was also similar and equal to 0.27±0.03 gPHA/gAcetate (COD basis).

3.3. Quantitative image analysis

Samples were taken during all accumulation experiments, fixed, and stained according to developed methods (Pei et al., 2022). The images were at 63X magnification assessed by CSLM with 11 random fields of view per well. The average of these 11 images was taken to represent average PHA to non-PHA biomass volume ratio. Floc to floc PHA distribution was found to be heterogeneous and variable. The correlation between the PHA to non-PHA biomass volume ratio and mass ratio was

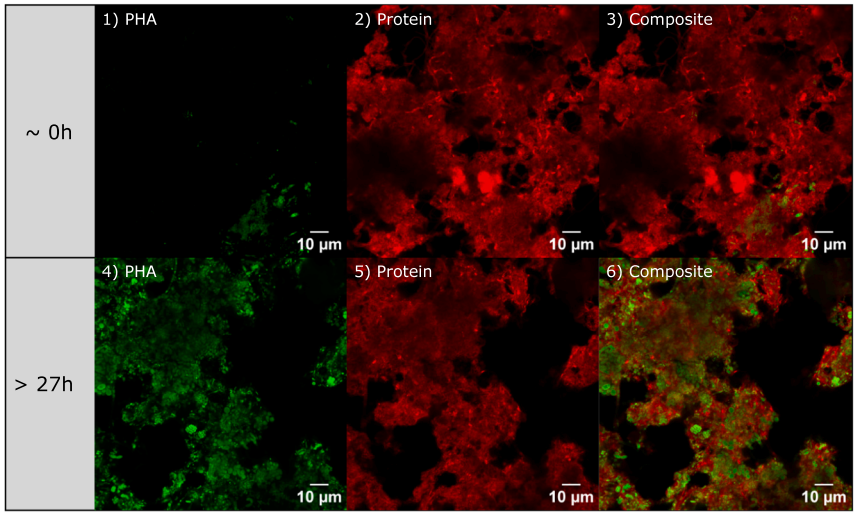

(a)

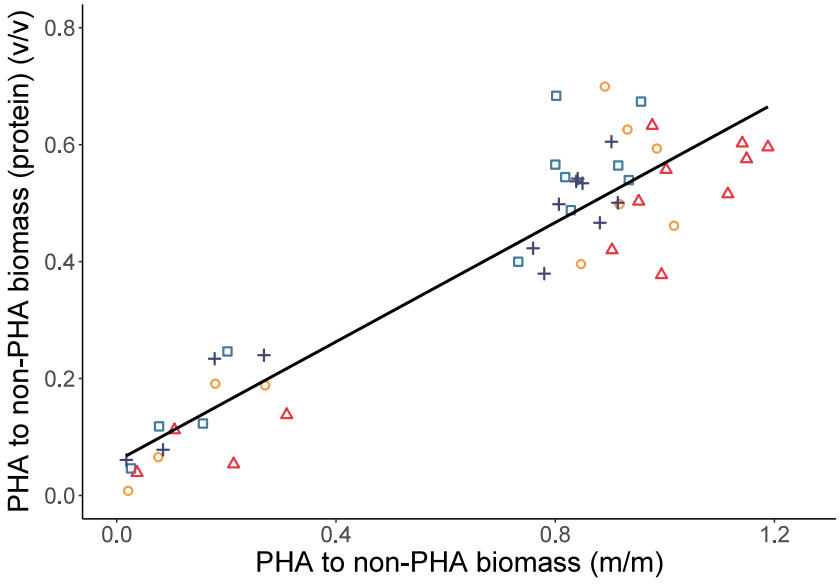

(b)

Fig. 5. Typical representations of staining image channels for PHA (green) and protein (red), plus the composite image at 63X magnifications **(a)** for activated sludge with low PHA to non-PHA biomass ratio (0 h) and high PHA to non-PHA biomass ratio (>27 h) accumulation. The average PHA to non-PHA biomass mass ratio and the volume ratio of PHA to non-PHA biomass (protein) measured by staining and Confocal Laser Scanning Microscope (CLSM) in 4 PHA accumulation replicated runs **(b)**. Blue□, yellow ○, red △ and purple + represent Run1, Run2, Run3 and Run4, respectively. The black line is the linear regression ($y = 0.51x + 0.06$, $R^2 = 0.86$) between PHA to non-PHA biomass mass ratio and the volume ratio of PHA to non-PHA biomass (protein). (For interpretation of the references to colour in this figure legend, the reader is referred to the web version of this article.)

assessed by Pearson correlation test. The Pearson correlation test showed that the ratio of PHA to non-PHA biomass volume represented by protein area (Cor = 0.90, DF = 46, $p < 0.001$) and DNA area (Cor = 0.81, DF = 45, $p < 0.001$) gave correspondence with PHA to non-PHA biomass mass ratio (Figs. 5 and 6).

The slope of the correlations is expected to be related to both measurement related factors as well as a density ratio conversion factor from v/v to w/w measurements. Different fluorophores have different characteristic imaging properties such as quantum yields. The outcome is that the more intense a signal the higher the probability that the fluorescence signal will diffuse and illuminate other surrounding Z stack layers of the floc structures. By CLSM, thin slices of the specimen are analyzed, with 1 Array unit setting for the CLSM, the integrated slice thickness depends directly also on the applied laser wavelength. Thus, as estimated in the appendix, the depth resolution decrease is in order of DAPI (258 nm), BODIPY (296 nm), SYPRO Red (355 nm) and Cy5 (388 nm). Measurement related factors may impose a systematic bias on the correlation, and they can also contribute to amplification of the observed variability depending on floc to floc differences in compactness.

Another factor that can affect the slope of the correlations is density differences between the PHA and non-PHA biomass. These differences generate a correction factor between the expressed mass ratio by TGA and the bio-volume ratios. The density of dried PHB powder is expected to be 1.25g/cm^3 and non-PHA biomass had a density of around 1.01g/cm^3 (Andreadakis, 1993; Peeters and Reynaers, 1994). However, the amorphous PHA and the nature of the PHA-rich biomass structures when hydrated is expected to influence density significantly. Neglecting the above mentioned laser dependent effects, volume ratio of PHA to non-PHA biomass (protein) correlation coefficient suggests that the PHA granules would be about half the density of the non-PHA biomass (Fig. 5). The suggested density difference would infer that for the downstream processing, the PHA-rich fraction of the biomass could be separated selectively by for example gradient centrifugation. More importantly, it suggested that the PHA could be harvested from the lighter fraction which agreed with Oshiki et al. (2010) where more PHA was recovered from the light fraction using buoyant density separation.

DNA staining and protein staining showed significant but also

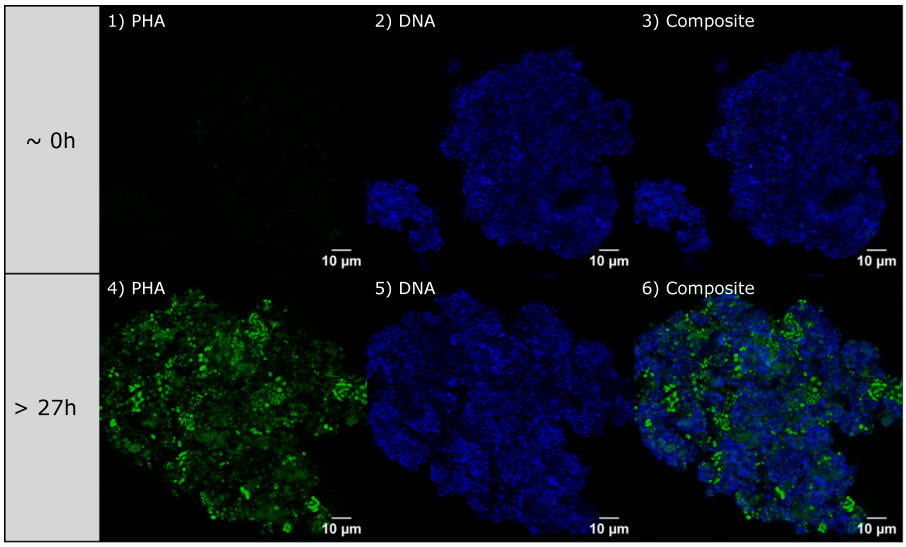

(a)

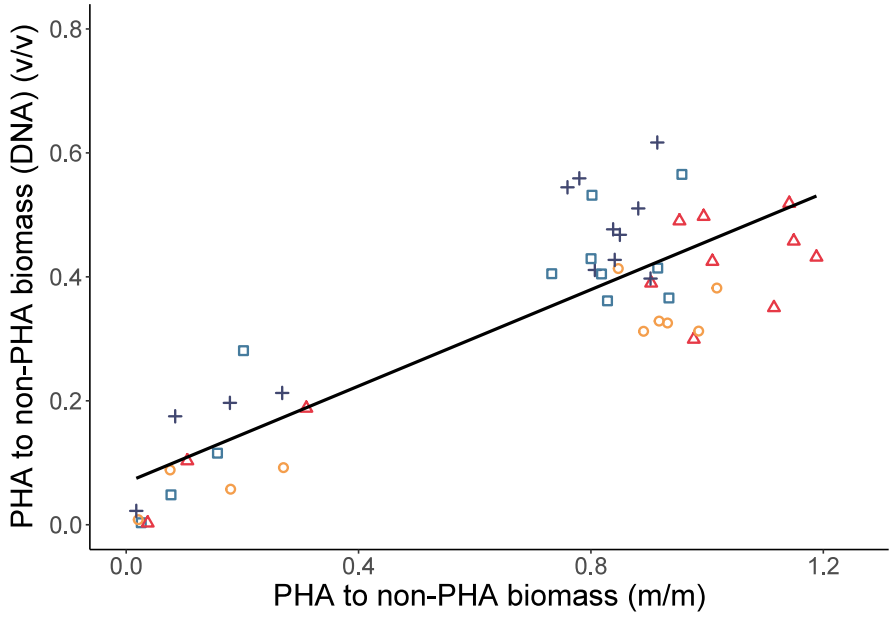

(b)

Fig. 6. Typical representations of staining image channels for PHA (green) and DNA (blue), plus the composite image at 63X magnifications **(a)** for activated sludge with low PHA to non-PHA biomass ratio (0 h) and high PHA to non-PHA biomass ratio (>27 h) accumulation. The average PHA to biomass mass m/m ratio versus the v/v ratio expressed by PHA area and DNA area **(b)**. Blue□, yellow ○, red △ and purple + represent Run1, Run2, Run3 and Run4, respectively. The black line is the linear regression ($y = 0.39x + 0.07$, $R^2 = 0.74$) between PHA to non-PHA biomass mass ratio and the volume ratio of PHA to non-PHA biomass (DNA). (For interpretation of the references to colour in this figure legend, the reader is referred to the web version of this article.)

different correlation constants in the v/v to w/w relationship. The PHA to non-PHA biomass ratio was considered to be more closely reflected by PHA area and protein area because cell protein is more abundant and is distributed more widely. Interestingly, development of intracellular PHA granules could be observed to take space in the cell cytoplasm and displace DNA (Pei et al., 2022). This effect was considered to be important especially when observing thicker floc structures. In these cases, PHA and DNA features were not well captured within the same focal plane affecting the representation the respective stained areas. However, overall, both the DNA and protein staining methods were capable of following the relative importance of v/v PHA accumulation in the biomass.

3.4. Degree of enrichment for PHA-storing microorganism

Both PHA to non-PHA biomass mass and volume ratios increased over time during the PHA accumulation process. At the later stage of the accumulation, stained PHA almost occupied the whole cell area to almost completely overlap with the biomass signal (Pei et al., 2022). Therefore, the volume ratio of PHA to non-PHA biomass at later stage was used to approximate the degree of enrichment for the PHA-storing biomass fraction.

Since the mass of PHA approached its extant maximum after 27 h accumulation (Fig. 4), results of v/v were pooled for an improved estimate of the degree of enrichment for PHA-storing microorganisms in the activated sludge. The degree of enrichment for PHA-storing microorganisms was estimated based on the applied staining pair, BODIPY with SYPRO Red or BODIPY with DAPI. The degree of enrichment estimated based on protein and DNA after 27 h, was found to be described by a normal distribution on the logit scale (Fig. 7). The average degree of enrichment (logit scale statistics) estimated based on protein for waste activated sludge from Bath WWTP was 55%. The range from the back transformed logit based standard deviation was between 47% to 62% v/v.

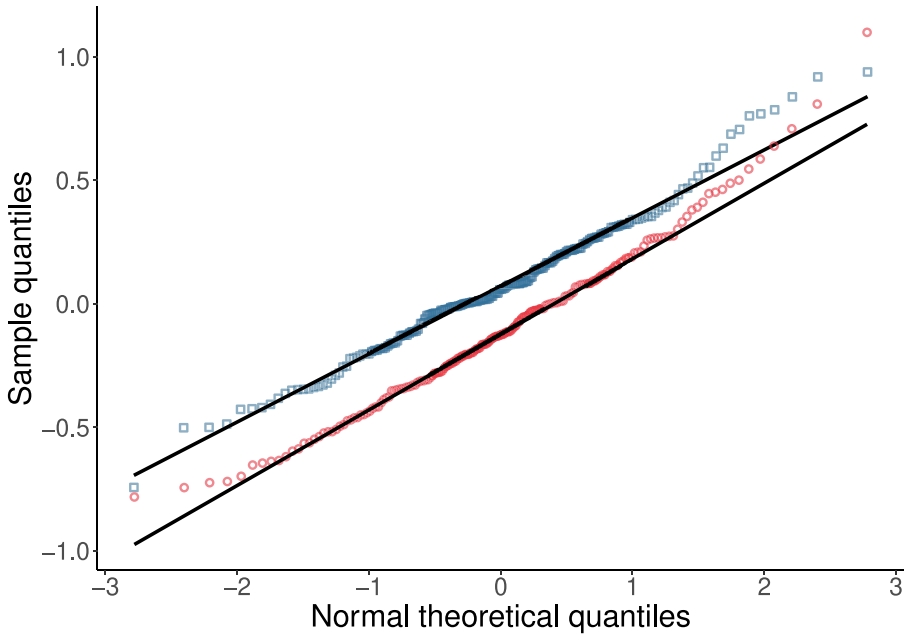

Fig. 7. Quantile-quantile plot for the pooled data of degree of enrichment identified with protein (blue□) and degree of enrichment identified with DNA (red ○)levels after 27 h on the logit scale.

The interpreted degree of enrichment for PHA-storing microorganisms of waste activated sludge from Bath WWTP indicates that only 55% of the biomass was accumulating PHA. This level is a significantly lower degree of enrichment compared to results reported for *enrichment accumulation* where the degree of enrichment was indicated up to almost 100% (Crognale et al., 2019). Therefore, waste activated sludge would perform better with *direct accumulation* if more of the organisms would accumulate PHA.

It has been suggested that possibilities to produce a better functional biomass in municipal activated sludge readily exist by methods to improve the stringency of disposing the biomass to periodic feast environments during the WWTP process (Morgan-Sagastume et al., 2014). Improvements in selection pressure without need for major process upgrades are expected to bring significant improvements in degree of enrichment without impacting on the core contaminants removal function of a WWTP. For example, it has been shown at pilot scale how more stringent anoxic feast (pre-denitrification for a BNR process) increased biomass PHA content from 0.15 gPHA/gVSS to 0.49 gPHA/gVSS (Bengsston et al., 2017). However, in this past work a distinction was not made between feast pressures to induce microbial community changes for PHA-storing microorganism enrichment versus performance of the PHA-storing microorganisms in the biomass. The methods of the present investigation enable to evaluate enrichment distinct from accumulation potential.

The observed heterogeneous nature of distribution of PHA in the sludge flocs is also informative towards development of efficient process strategies to recover the polymers. This work found that 45% of the biomass was void of polymer. Research efforts have been applied previously to upgrade a PHA-rich biomass based on density differences. Selective protein digestion, or mild non-specific oxidative treatment of the floc structures may also be expected to be effective pre-treatment if the non-PHA biomass fractions are more selectively influenced. At the same time, stress imposed on the biomass is known to promote polymer degradation. This risk for losses must be considered at the same time (Obruca et al., 2018). The advantage of selective staining methods is that such pre-treated biomass may also be evaluated towards a qualitative or quantitative impression of the morphological influence as a function of pre-treatment severity.

3.5. The PHA-storing fraction

The estimated average PHA content in PHA-accumulating fraction was defined as follows:

$$\frac{\text{Biomass PHA content}}{\text{Biomass PHA content} + \text{DE}\cdot\text{Non-PHA biomass}} \tag{7}$$

where Biomass PHA content after 3τ is used and DE is the degree of enrichment defined by Eq. (2). In the present study, average biomass PHA content for the PHA-storing fraction in the activated sludge was equal to 0.64 ± 0.04 gPHA/gVSS.

The estimated average PHA accumulation capacity for the PHA-storing fraction in these *direct accumulation* experiments was higher than the PHA accumulation capacity found for *enrichment accumulation* reported by Valentino et al. (2019). However, the average PHA accumulation capacity for the PHA-storing fraction found in these *direct accumulations* was still lower than the more functionalized *enrichment accumulation* methods that select for *Plasticicumulans acidivorans* (Johnson et al., 2009). Therefore, the PHA accumulation capacity for the selected PHA-storing bacteria also influences the PHA accumulation potential.

These differences of the PHA accumulation capacity in both *enrichment* and *direct* accumulation suggested that selection of PHA-storing microorganisms does not necessarily mean the selection of the accumulators with high PHA accumulation potential. Therefore, the function of the selection needs to be further understood and clarified without ambiguity with respect to effects of both degree of enrichment and PHA accumulation capacity for the PHA-storing fraction in the biomass.

Selection and resultant phenotype potential is one aspect of expressing a high biomass PHA content in a microbial community. Physiological state has also been reported to be of influence to the expressed biomass PHA content for given microorganisms or microbial communities (Morgan-Sagastume et al., 2017; Obruca et al., 2017). A given feast-famine regime or feed on demand strategy may be applied which induces optimum response for PHA accumulation. Often there are small differences in operational conditions that are not considered explicitly in reported comparisons of results. These differences may include biomass history in the WWTP before the accumulation process. Specific details also include the substrate supply during the

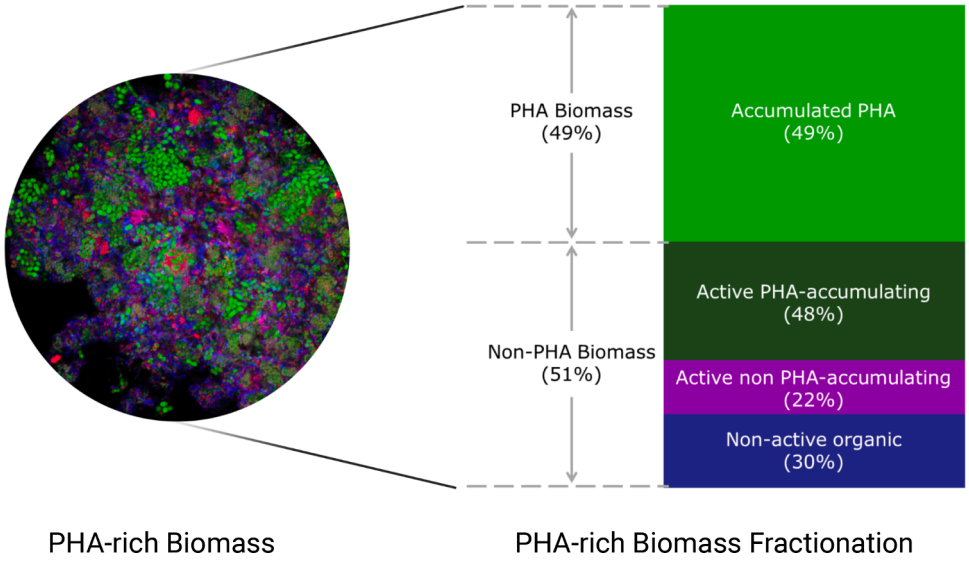

Fig. 8. The PHA-rich biomass fractionation based on the staining of PHA (green), RNA (red) and DNA (blue). The figure was created with *BioRender.com*.

accumulation process, background substrate levels during the accumulation process, the sizes or concentration of the pulses, and acclimation. Insights from evaluations based only on the end-point biomass PHA content are limited without reference to degree of enrichment. Therefore, it is important to incorporate the methods like selective staining to elucidate deepened understanding of operational conditions on the maximum biomass PHA content.

3.6. Quantification of the dynamics of microbial activity expressed by 16S rRNA

Dynamics of microbial activity were assessed by FISH targeting at 16S rRNA incorporated with PHA staining and non-PHA biomass counter staining. The area ratio between RNA and DNA was used to represent the viable bacteria fraction (Eq. (3)). In the *direct accumulation* process, the viable bacteria fraction identified from individual fields of view at 63X magnification showed significant differences during the accumulation process (DF = 12, Residue = 568, $F = 12.04$, $p < .001$). This significant difference suggested that within the biomass, the microbial activity is distributed heterogeneously among flocs.

The average activity for the biomass was calculated by making an average of the RNA to DNA ratio for 11 fields of view from one well with 63X magnification. This average activity for the biomass did not follow a measurable trend during the whole accumulation process (DF = 12, Residue = 34, $F = 1.503$, $p = 0.171$). The interpreted average microbial activity levels for the biomass were stable, without correlation to time within the precision of these evaluations. A specific activity level influence of acclimation before accumulation was also not found. To increase the resolution of the methods, it is necessary to identify PHA accumulation activity level at the cellular level. This level of identification would require techniques such as applying qPCR to the expressed PhaC gene, FISH targeting at mRNA of PhaC, or BONCAT-FISH targeting at expressed PHA polymerise proteins.

The staining tools in combination with FISH could be applied to follow the dynamic nature of the biomass and discriminate between active PHA-accumulating, active non PHA-accumulating and non-active organic fractions of the activated sludge. In the waste activated sludge collected from Bath WWTP, based on the replicate experiments of distinct batches, the activated sludge was fractionated. The average viable biomass fraction during the whole accumulation process (evaluated on the logit scale) was 70% with a range from the back transformed logit standard deviation of 52% to 83% RNA/DNA. The area ratio between PHA and RNA was used to represent the PHA-accumulating fraction of the viable biomass (Eq. (4)). It was found that 68% (PHA/RNA) of the active biomass was accumulating PHA. Combining the size of active biomass fraction and its PHA-accumulating fraction, it was estimated that 48% of non-PHA biomass (based on DNA staining) was actively accumulating PHA. Therefore, as shown in Fig. 8, the non-PHA biomass for activated sludge from Bath WWTP could be fractionated into 48% of active PHA-accumulating fraction, 22% of active non PHA-accumulating fraction and 30% non-active organic fraction. The active non PHA-storing fraction dilutes not only the biomass PHA content but also consumes substrates and oxygen. This active flanking population could contribute to lowering PHA yield, and overall process performance/productivity.

4. Conclusions

- Quantitative image analysis methods for evaluating PHA storing microbial communities have been developed. They allow for the estimation of the PHA storing bacteria fraction and the average PHA content of the PHA storing bacteria.
- The waste activated sludge used in these *direct accumulation* experiments expressed a degree of enrichment of 55% (47%-62%).
- The PHA in the activated sludge was diluted by flanking biomass. The estimated average biomass PHA content for the PHA-storing biomass fraction was 0.64 ± 0.04 gPHA/gVSS.
- *Enrichment accumulation* approach has higher degree of enrichment but is not necessarily enriching bacteria that express a higher PHA accumulation capacity compared to *direct accumulation*.
- Selection has two components: to improve the degree of enrichment and to promote conditions to select PHA-storing bacteria with a higher PHA accumulation capacity.
- Microbial activities in the total biomass were relatively constant during the accumulation process and 68% of active bacteria were estimated to be accumulating PHA. This outcome confirmed the existence of viable flanking microbial population which may consume added substrate and generate additional oxygen demand in a PHA accumulation process.

Declaration of Competing Interest

The authors declare that they have no known competing financial interests or personal relationships that could have appeared to influence the work reported in this paper.

Data Availability

Data will be made available on request.

Acknowledgment

This work was performed in the cooperation framework of Wetsus, European Centre of Excellence for Sustainable Water Technology (www.wetsus.nl). Wetsus is co-funded by the Dutch Ministry of Economic Affairs and Ministry of Infrastructure and Environment, the European Union Regional Development Fund, the Province of Fryslân and the Northern Netherlands Provinces. This research has received funding from the European Union's Horizon 2020 research and innovation programme under the grant agreements No 817788 and No 101036838. The authors thank the participants and industrial/public partners (Paques Biomaterials BV, STOWA, and SNB) of the research theme "Biopolymers from water" for fruitful discussions and financial support. The authors also thank Erik de Vries, Francisca Braga, Deimante Misiukonyte, Leonora Hibic Burtina, John Ferwerda and the technical department of Wetsus for the help of operating the PHA accumulation pilot. The authors thank the meaningful discussion with Angel Estevez Alonso and Agnieszka Tomaszewska. The graphical abstract and Figure 8 in this work was created with *BioRender.com*.

Appendix A

According to the manual of Zeiss for LSM 880, while using 1 Array Unit, the optical slice thickness and axial resolution are identical. This is often referred as depth resolution and can be calculated with the following equation with a correction factor of 0.87:

$$\frac{0.64 \times \overline{\lambda}}{n - \sqrt{n^2 - NA^2}}$$

Where, $\overline{\lambda} = \sqrt{2}\,\frac{\lambda_{Ex}+\lambda_{Em}}{\sqrt{\lambda_{Ex}^2+\lambda_{Em}^2}}$, could be simplified as $\overline{\lambda} = \sqrt{\lambda_{Ex} \times \lambda_{Em}}$;

n: refraction index;

NA: numerical aperture.

The depth resolution was estimated for the dyes while using objective 63X/1.4 Oil DIC M27 that $NA = 1.4$. In this case, the applied immersion oil Immersol 518 F (Carl Zeiss, Germany) had a refraction index $n = 1.518$. For the estimation of the $\overline{\lambda}$, the wavelength of the laser for exciting the respective dye was used as λ_{Ex} and the maximum emission reported by the manufacture was used as λ_{Em}. The estimated $\overline{\lambda}$ and depth resolution are summarized in the following Table A.1:

Table A.1
The estimated depth resolution for DAPI, BODIPY, SYPRO Red and Cy5 using objective 63X/1.4 Oil DIC M27 in combination with immersion oil Immersol 518 F.

	Ex (nm)	Em (nm)	$\overline{\lambda}$ (nm)	Depth resolution (nm)
DAPI	405	461	432	258
BODIPY	488	503	495	296
SYPRO Red	561	630	594	355
Cy5	633	666	649	388

References

Anderson, A.J., Dawes, E.A., 1990. Occurrence, Metabolism, Metabolic Role, and Industrial Uses of Bacterial Polyhydroxyalkanoates. Technical Report 4.http://mmbr.asm.org/

Andreadakis, A.D., 1993. Physical and chemical properties of activated sludge floc. Water Res. 27 (12), 1707–1714. https://doi.org/10.1016/0043-1354(93)90107-S.

Bengsston, S., Werker, A., Visser, C., Korving, L., 2017. PHARIO Stepping Stone to a Sustainable Value Chain for PHA Bioplastic using Municipal Activated Sludge. Report 2017-15. STOWA.93

Bengtsson, S., Werker, A., Visser, C., Korving, L., 2017. PHARIO Stepping Stone To A Sustanable Value Chain For PHA Bioplastics Using Municipal Activated Sludge. Technical Report 2017-15. STOWA, Amersfort, the Netherlands. ISBN 978.90.5773.752.7

Chan, C.M., Johansson, P., Magnusson, P., Vandi, L.-J.J., Arcos-Hernandez, M., Halley, P., Laycock, B., Pratt, S., Werker, A., L-j, V., 2017. Mixed culture polyhydroxyalkanoate-rich biomass assessment and quality control using thermogravimetric measurement methods. Polym. Degrad. Stab. 144, 110–120. https://doi.org/10.1016/j.polymdegradstab.2017.07.029.

Crognale, S., Tonanzi, B., Valentino, F., Majone, M., Rossetti, S., 2019. Microbiome dynamics and phaC synthase genes selected in a pilot plant producing polyhydroxyalkanoate from the organic fraction of urban waste. Sci. Total Environ. 689, 765–773. https://doi.org/10.1016/j.scitotenv.2019.06.491.

Dawes, E.A., Senior, P.J., 1973. The role and regulation of energy reserve polymers in micro-organisms. Adv. Microb. Physiol. 10, 135–266. https://doi.org/10.1016/S0065-2911(08)60088-0.

Estevez-Alonso, A., Pei, R., van Loosdrecht, M.C., Kleerebezem, R., Werker, A., 2021. Scaling-up microbial community-based polyhydroxyalkanoate production: status and challenges. Bioresour. Technol. 327, 124790. https://doi.org/10.1016/j.biortech.2021.124790.

Johnson, K., Jiang, Y., Kleerebezem, R., Muyzer, G., Van Loosdrecht, M.C.M., 2009. Enrichment of a mixed bacterial culture with a high polyhydroxyalkanoate storage capacity. Biomacromolecules 10 (4), 670–676. https://doi.org/10.1021/bm8013796.

Kacmar, J., Carlson, R., Balogh, S.J., Srienc, F., 2006. Staining and quantification of poly-3-hydroxybutyrate in Saccharomyces cerevisiae and Cupriavidus necator cell populations using automated flow cytometry. Cytom. Part A 69A (1), 27–35. https://doi.org/10.1002/cyto.a.20197.

Kleerebezem, R., van Loosdrecht, M.C.M., 2007. Mixed culture biotechnology for bioenergy production. Curr. Opin. Biotechnol. 18 (3), 207–212. https://doi.org/10.1016/j.copbio.2007.05.001.

Kourmentza, C., Plácido, J., Venetsaneas, N., Burniol-Figols, A., Varrone, C., Gavala, H. N., Reis, M.A.M., 2017. Recent advances and challenges towards sustainable polyhydroxyalkanoate (PHA) production. Bioengineering 4 (2), 55. https://doi.org/10.3390/bioengineering4020055.http://www.mdpi.com/journal/bioengineeringhttp://www.mdpi.com/2306-5354/4/2/55

Laycock, B., Halley, P., Pratt, S., Werker, A., Lant, P., 2013. The chemomechanical properties of microbial polyhydroxyalkanoates. Prog. Polym. Sci. 38 (3–4), 536–583. https://doi.org/10.1016/j.progpolymsci.2012.06.003.

Llobet-Brossa, E., Rosselló-Mora, R., Amann, R., 1998. Microbial community composition of Wadden sea sediments as revealed by fluorescence *in situ* hybridization. Appl. Environ. Microbiol. 64 (7), 2691–2696. https://doi.org/10.1128/aem.64.7.2691-2696.1998.

Majed, N., Matthäus, C., Diem, M., Gu, A.Z., 2009. Evaluation of intracellular polyphosphate dynamics in enhanced biological phosphorus removal process using Raman microscopy. Environ. Sci. Technol. 43 (14), 5436–5442. https://doi.org/10.1021/ES900251N.

Majone, M., Dircks, K., Beun, J.J., 1999. Aerobic storage under dynamic conditions in activated sludge processes. The state of the art. Water Sci. Technol. 39 (1), 61–73. https://doi.org/10.1016/S0273-1223(98)00776-8.

Morgan-Sagastume, F., 2016. Characterisation of open, mixed microbial cultures for polyhydroxyalkanoate (PHA) production. Rev. Environ. Sci. Biotechnol. 15 (4), 593–625. https://doi.org/10.1007/s11157-016-9411-0.

Morgan-Sagastume, F., Valentino, F., Hjort, M., Cirne, D., Karabegovic, L., Gerardin, F., Johansson, P., Karlsson, A., Magnusson, P., Alexandersson, T., Bengtsson, S.,

Majone, M., Werker, A., 2014. Polyhydroxyalkanoate (PHA) production from sludge and municipal wastewater treatment. Water Sci. Technol. 69 (1), 177–184. https://doi.org/10.2166/wst.2013.643.

Morgan-Sagastume, F., Valentino, F., Hjort, M., Zanaroli, G., Majone, M., Werker, A., 2017. Acclimation process for enhancing polyhydroxyalkanoate accumulation in activated-Sludge biomass. Waste Biomass Valorization 10 (4), 1–18. https://doi.org/10.1007/s12649-017-0122-8.

Obruca, S., Sedlacek, P., Koller, M., Kucera, D., Pernicova, I., 2018. Involvement of polyhydroxyalkanoates in stress resistance of microbial cells: biotechnological consequences and applications. 10.1016/j.biotechadv.2017.12.006.

Obruca, S., Sedlacek, P., Mravec, F., Krzyzanek, V., Nebesarova, J., Samek, O., Kucera, D., Benesova, P., Hrubanova, K., Milerova, M., Marova, I., 2017. The presence of PHB granules in cytoplasm protects non-halophilic bacterial cells against the harmful impact of hypertonic environments. New Biotechnol. 39, 68–80. https://doi.org/10.1016/j.nbt.2017.07.008.

Oshiki, M., Onuki, M., Satoh, H., Mino, T., 2010. Separation of PHA-accumulating cells in activated sludge based on differences in buoyant density. J. Gen. Appl. Microbiol. 56 (2), 163–167. https://doi.org/10.2323/jgam.56.163.

Paul, E., Bessière, Y., Dumas, C., Girbal-Neuhauser, E., 2020. Biopolymers production from wastes and wastewaters by mixed microbial cultures: strategies for microbial selection. 10.1007/s12649-020-01252-6.

Peeters, J., Reynaers, M., 1994. Crystallization phenomena in bacterial poly[(R)-3-hydroxybutyrate]: 3. Toughening via texture changes. Polymer 35 (21), 4598. https://doi.org/10.1016/0032-3861(94)90809-5.

Pei, R., Vicente-Venegas, G., Tomaszewska, A., Van Loosdrecht, M. C. M., Kleerebezem, R., Werker, A., 2022. Visualisation of polyhydroxyalkanoate accumulated in waste activated sludge. Submitted.

Pratt, S., Vandi, L.J., Gapes, D., Werker, A., Oehmen, A., Laycock, B., 2019. Polyhydroxyalkanoate (PHA) bioplastics from organic waste. Biorefinery 615–638. https://doi.org/10.1007/978-3-030-10961-5_26.

Reis, M.A.M., Serafim, L.S., Lemos, P.C., Ramos, A.M., Aguiar, F.R., Van Loosdrecht, M.C. M., 2003. Production of polyhydroxyalkanoates by mixed microbial cultures. Bioprocess. Biosyst. Eng. 25 (6), 377–385. https://doi.org/10.1007/s00449-003-0322-4.

Saranya, V., Poornimakkani, Krishnakumari, M.S., Suguna, P., Binuramesh, C., Abirami, P., Rajeswari, V., Ramachandran, K.B., Shenbagarathai, R., 2012. Quantification of intracellular polyhydroxyalkanoates by virtue of personalized flow cytometry protocol. Curr. Microbiol. 65 (5), 589–594. https://doi.org/10.1007/s00284-012-0198-0.

Tamis, J., Lužkov, K., Jiang, Y., Loosdrecht, M.C., Kleerebezem, R., 2014. Enrichment of plasticicumulans acidivorans at pilot-scale for PHA production on industrial wastewater. J. Biotechnol. 192 (Part A), 161–169. https://doi.org/10.1016/j.jbiotec.2014.10.022.

Valentino, F., Lorini, L., Pavan, P., Bolzonella, D., Majone, M., 2019. Organic fraction of municipal solid waste conversion into polyhydroxyalkanoates (PHA) in a pilot scale anaerobic/aerobic process. Chem. Eng. Trans. 74 (March 2018), 265–270. https://doi.org/10.3303/CET1974045.

Valentino, F., Morgan-Sagastume, F., Campanari, S., Villano, M., Werker, A., Majone, M., 2017. Carbon recovery from wastewater through bioconversion into biodegradable polymers. New Biotechnol. 37, 9–23. https://doi.org/10.1016/j.nbt.2016.05.007.

Van Loosdrecht, M.C.M., Pot, M.A., Heijnen, J.J., 1997. Importance of bacterial storage polymers in bioprocesses. Water Sci. Technol. 35 (1), 41–47. https://doi.org/10.1016/S0273-1223(96)00877-3.

Vidal-Mas, J., Resina-Pelfort, O., Haba, E., Comas, J., Manresa, A., Vives-Rego, J., 2001. Rapid flow cytometry - Nile red assessment of PHA cellular content and heterogeneity in cultures of pseudomonas aeruginosa 47T2 (NCIB 40044) grown in waste frying oil. Antonie van Leeuwenhoek 80 (1), 57–63. https://doi.org/10.1023/A:1012208225286.

Warton, D.I., Hui, F.K.C., 2011. The arcsine is asinine: the analysis of proportions in ecology. Ecology 92 (1), 3–10.

Werker, A., Bengtsson, S., Johansson, P., Magnusson, P., Gustafsson, E., Hjort, M., Anterrieu, S., Karabegovic, L., Alexandersson, T., Karlsson, A., Morgan-Sagastume, F., Sijstermans, L., M, T., Wypkema, E., van der Kooij, Deeke, A.Y., Uijterlinde, C., Korving, L., 2020. Production quality control of mixed culture poly (3-hydroxbutyrate-co-3-hydroxyvalerate) blends using full-scale municipal activated sludge and non-chlorinated solvent extraction. In: Koller, M. (Ed.), The Handbook of Polyhydroxyalkanoates, Vol. 2. CRC Press, Oxon (UK) and Boca Raton (FL, USA). (Kinetic)